

## Supplementary Information

### Construction of Catalytic Cavities in Porous Aromatic Frameworks for Effective Alcohol Oxidation

Yuhui Zhai, Hengtao Lei, Yue Li, Jian Song, Xiaofei Jing, Xiaoyuan Shi\*, Yuyang Tian\* and  
Guangshan Zhu

#### Contents

- 1 General methods
- 2 Characterizations of PAF-278 and PAF-279
- 3 Catalysis performance of PAF-279
- 4 Synthesis of Compound I and Compound II
- 5 Characterization of Compound I and Compound II
- 6 Catalysis performance of Compound II
- 7  $^1\text{H}$  NMR spectra of organic compound
- 8 GC spectra and mass spectrometry

## 1 General methods

FTIR was performed as KBr pellets using a Shimadzu-Prestige 21 Fourier transform infrared spectrometer. TGA was recorded by a METTLER TOLEDO TGA/DSC 2 thermal analyzer under nitrogen atmosphere at the heating rate of  $10\text{ }^{\circ}\text{C min}^{-1}$ . XPS was taken on a K-Alpha XPS spectrometer (Thermo Scientific K-Alpha). SEM analysis was examined on a JEOL JSM 6700 system. TEM was obtained on a JEOL JEM 3010 instrument with an accelerating voltage of 200 kV.  $\text{N}_2$  adsorption isotherms and pore size distribution were tested on a Autosorb iQ2 adsorptometer, Quantachrome Instrument. CHN element analysis was conducted using CHN Elemental Analyzer from PerkinElmer 2400. The EPR spectra were obtained on a JES-FA 200 EPR spectrometer. Conversion and selectivity was examined on thermo scientific ISQ 7000.

## 2 Characterizations of PAF-278 and PAF-279

**Table.S1** Elemental analytical content of CNH of PAF-279.

	C	N	H
Theoretical	87.91	2.36	7.04
Experimental	85.466	2.24	3.42

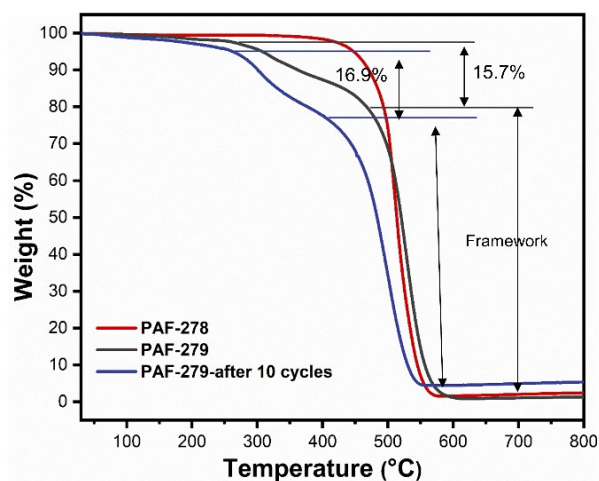


**Figure. S1** TGA of PAF-278 (red), PAF-279 (gray), PAF-279 after 10 cycles(blue).

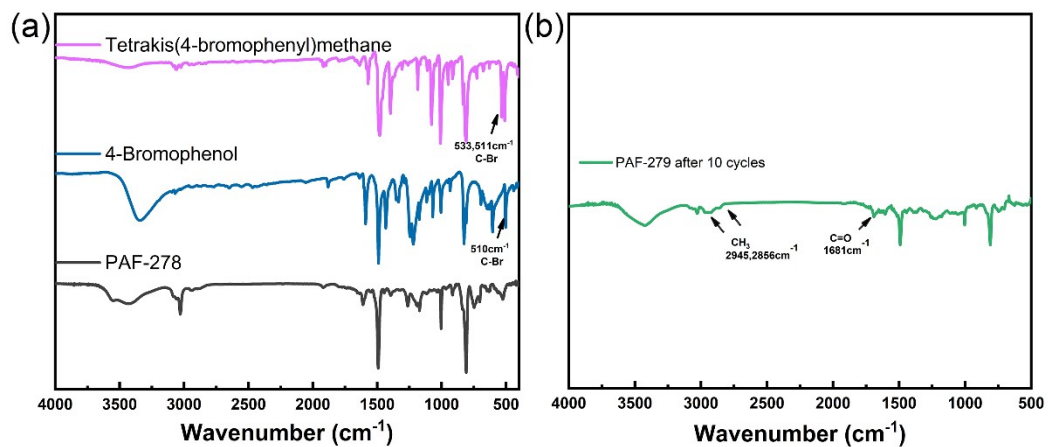


Figure. S2 (a) IR of PAF-278, (b) PAF-279 after 10 cycles.

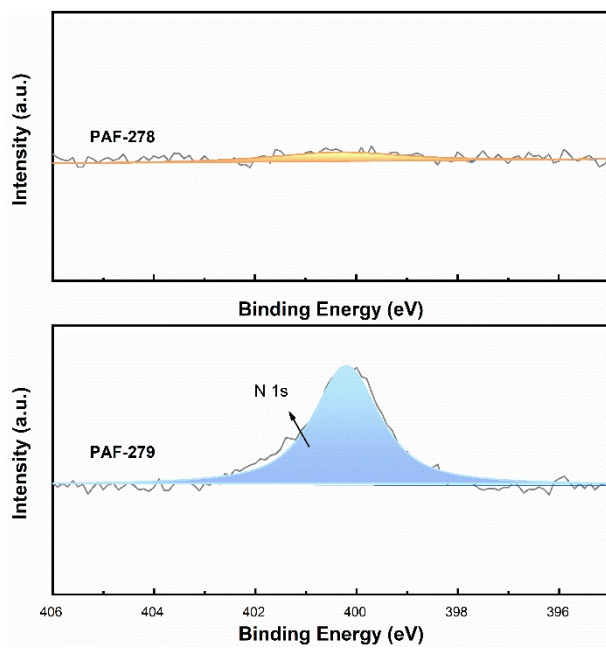
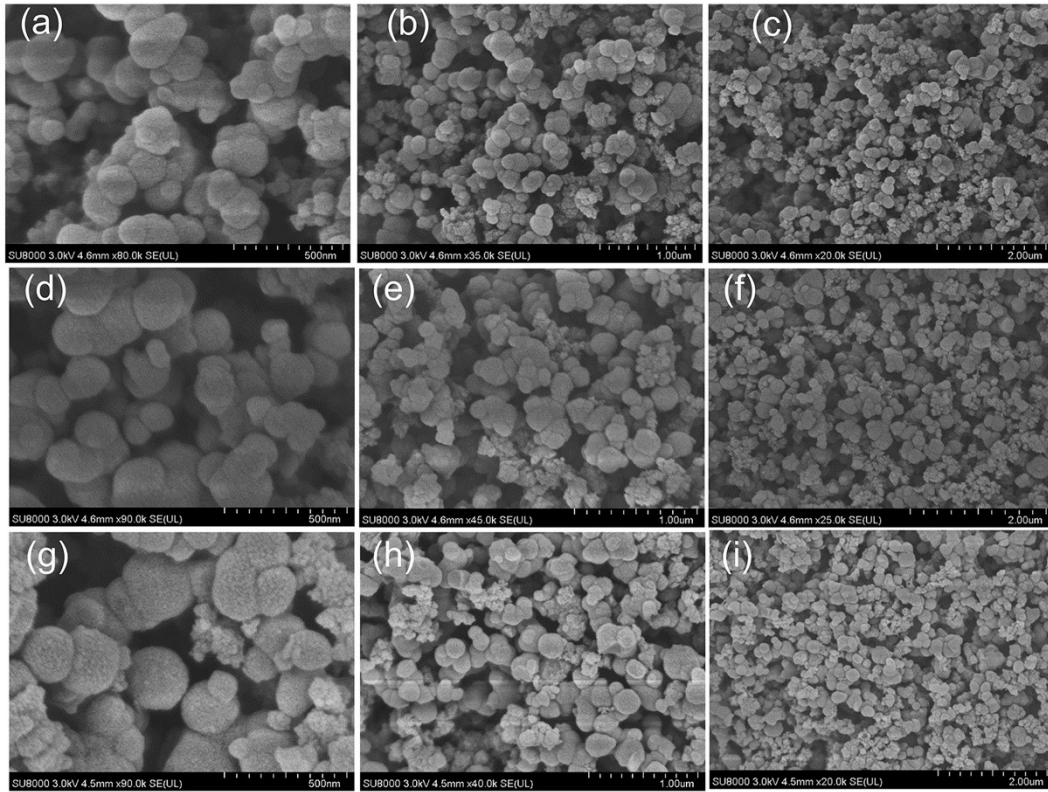
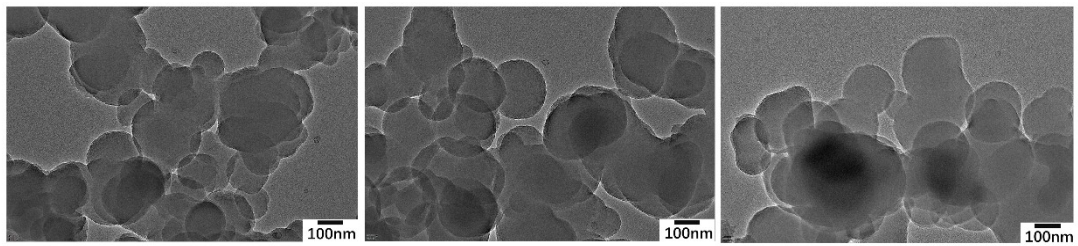


Figure. S3 N 1s spectra of PAF-278 and PAF-279.



**Figure. S4** SEM images of PAF-278 (a-c), for PAF-279 (d-f), for PAF-279 after 10 cycles (g-i).



**Figure. S5** TEM images of PAF-279.

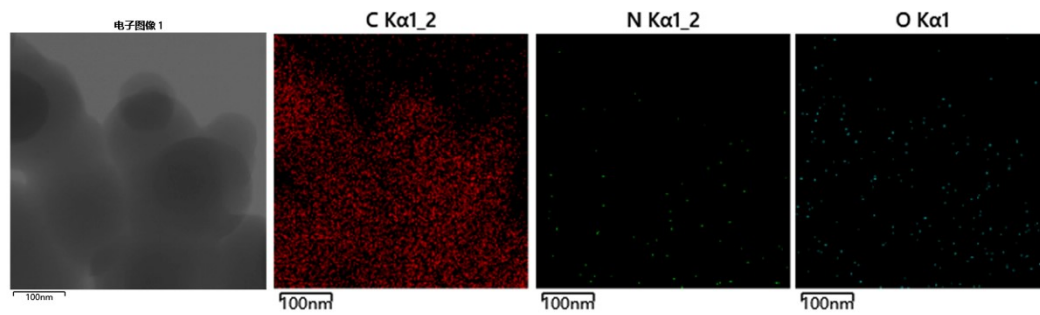


**Figure. S6** EDS mapping of PAF-279.

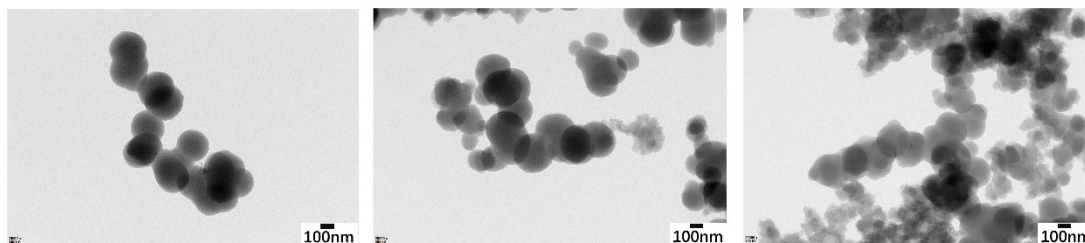


**Figure. S7** TEM images of PAF-279 after 10 cycles.

**Table.S2** Elemental analytical content of CNH.

	<b>C</b>	<b>N</b>	<b>H</b>
PAF-279	85.466	2.24	3.42
PAF-279 after 10 cycles	90.02	2.288	7.2

### 3. Catalysis performance of PAF-279

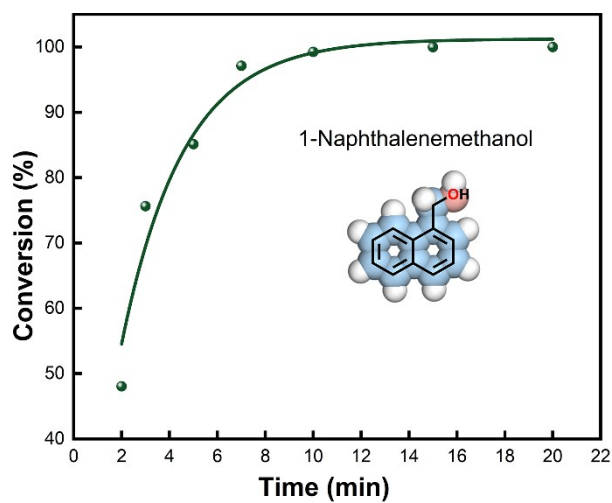


**Figure. S8** Conversion curve for 1-Naphthalenemethanol.

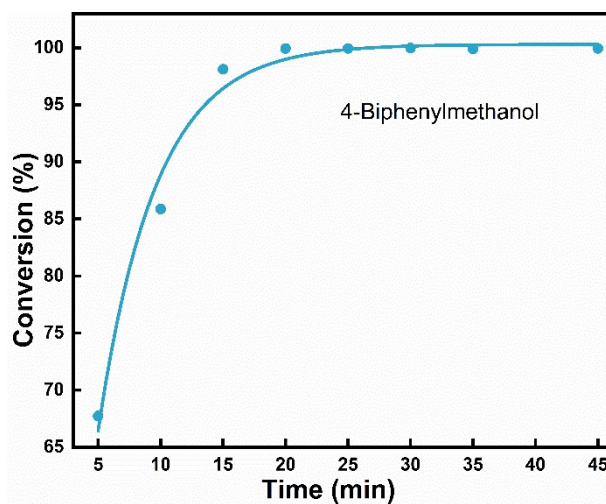


Figure. S9 Conversion curve for 4-Biphenylmethanol at room temperature.

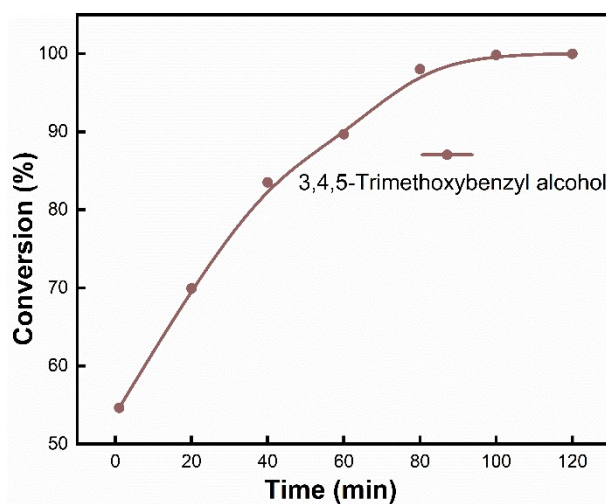


Figure. S10 Conversion curve for 3,4,5-Trimethoxybenzyl alcohol at room temperature.

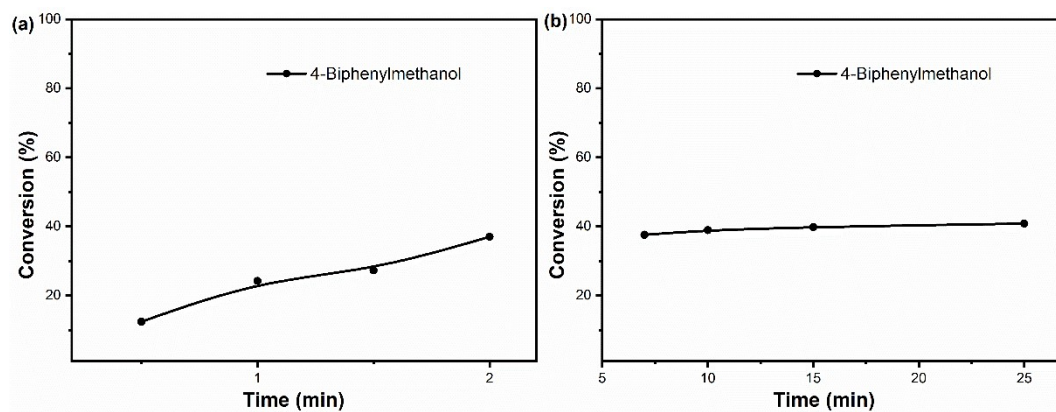
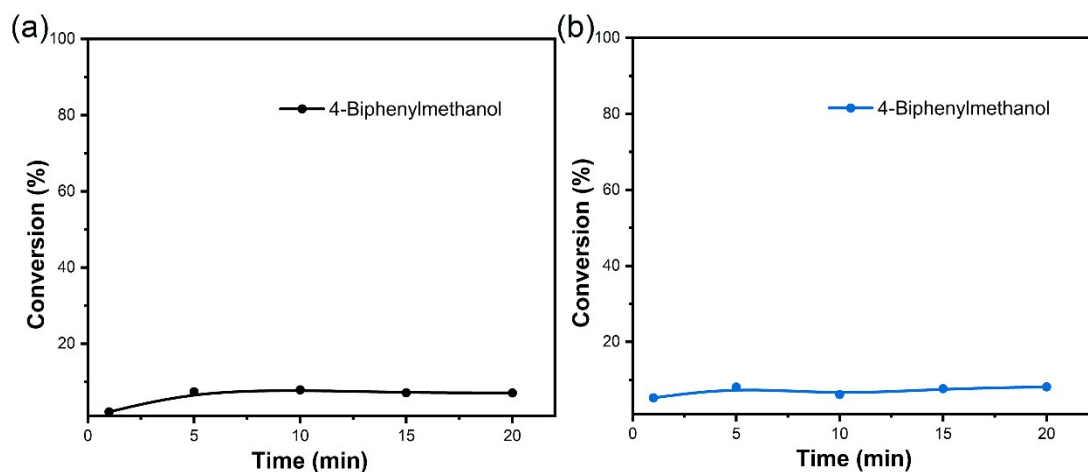
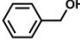
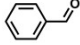
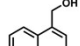
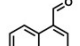
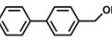
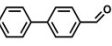
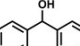
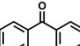
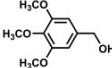
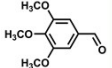


Figure. S11 Conversion curve for 4-Biphenylmethanol with PAF-279 (a) and the solution was filtered to remove the PAF-279 (b)



**Figure. S12** Conversion curve for 4-Biphenylmethanol without any catalyst (a) and with the existence of PAF-278 (b).

**Table. S3** TOF of alcohols at 45°C.

Entry	Substrate	Product	TOF[h <sup>-1</sup> ]
1			174.4
2			120
3			150
4			27
5			80

**Table S4.** Comparison of catalytic activities on oxidation of benzyl alcohol. The turnover frequency (TOF) was calculated based on the amount of (Cl-acetamido)-TEMPO in the PAF-279 as TOF = moles of desired product formed/moles of catalyst/reaction time.

Cat.	Oxidant	TOF [h <sup>-1</sup> ]	ref
PAF-279	O <sub>2</sub>	171.4	Our work
JUC-566	O <sub>2</sub>	132	1
MNST	O <sub>2</sub>	125	2
SBA-15-ABNO	O <sub>2</sub>	111	3
TEMPO	Air	100	4
SBA-15-supported TEMPO	O <sub>2</sub>	66.7	5
TEMPO-CMP-4	O <sub>2</sub>	40	6
IL@SBA-15-TEMPO	O <sub>2</sub>	28.57	7

TEMPO/HBPEK	O <sub>2</sub>	23	8
TEMPO@Fe <sub>3</sub> O <sub>4</sub>	O <sub>2</sub>	20	9
UiO-67-TEMPO (38%)	O <sub>2</sub>	19.2	10
TEMPO-coated SPN catalyst 5b	Air	17	11
UiO-68-TEMPO	Air	2.5	12
DPIO	O <sub>2</sub>	1.1	13
PPO-TEMPO	HClO	200	14
HPAF-TEMPO	air	3.2	15
FDU-15-TEMPO	NaClO	467	16

#### 4. Synthesis of Compound I and Compound II

Compound I was synthesized via palladium-catalyzed Sonogashira–Hagihara cross-coupling reaction. Typically, tetrakis(4-ethynylphenyl)methane (209 mg, 0.5 mmol), 2,5-Dibromobenzene-1,4-diol (267.9 mg, 1 mmol), tetrakis(triphenylphosphine)palladium (63 mg), and copper iodide (23 mg) were dissolved in a mixture of DMF (15 mL) and Et<sub>3</sub>N (15 mL) in a 100 mL flask. After degassing via three freeze-pump-thaw cycles, the mixture was stirred at 100°C for 48 h under a N<sub>2</sub> atmosphere. After cooling down to room temperature, the resulting Compound II was collected by filtration, followed by consecutive washing with N,N-Dimethylformamide (50 mL), 1M HCl (100 mL), methanol (50 mL), and acetonitrile (50 mL) to remove the unreacted monomers and catalysts.

50 ml flask was charged with Compound I (100 mg), K<sub>2</sub>CO<sub>3</sub> (300 mg), 4-(2-Chloroacetamido)-TEMPO (80 mg) and anhydrous acetonitrile (20 mL). The flask was sealed and heated at 80°C for 2 days. The resulting solid was collected, washed with HCl (2M), DI water, and methanol, then dried under vacuum to produce Compound II as black powder.



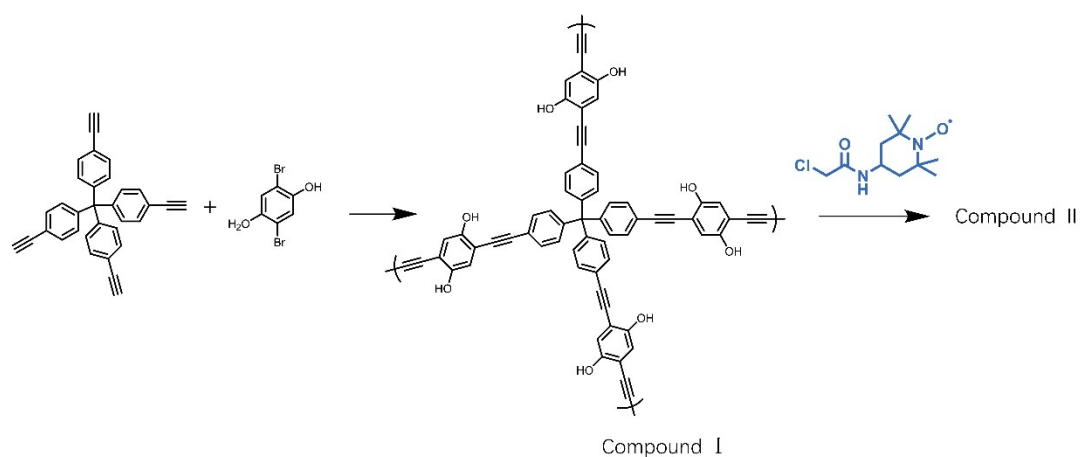


**Figure. S13** Synthetic routes of the functionalized Compound II.<sup>17-18</sup>

### 5. Characterization of Compound I and Compound II

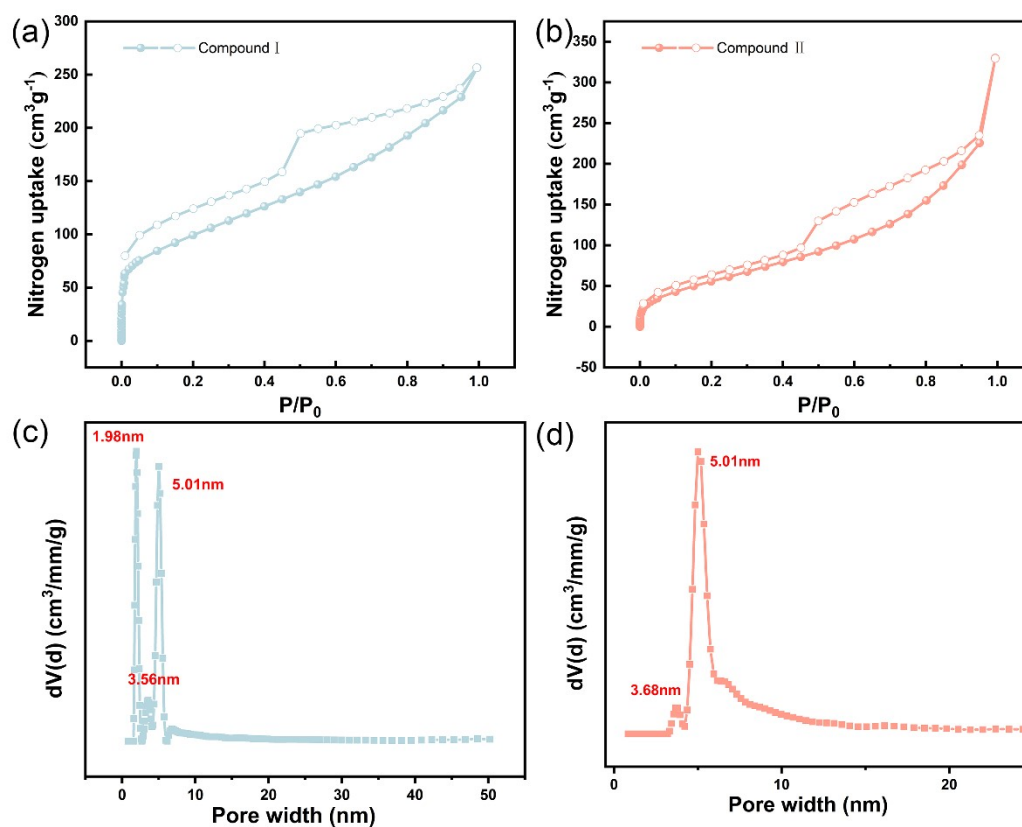


**Figure. S14** Nitrogen adsorption and desorption isotherms and pore size distribution of Compound I and Compound II.

Table. S5 Pore porosity of Compound I and Compound II.

	BET surface area (m <sup>2</sup> /g) total/micro-	Pore volume (cm <sup>3</sup> g <sup>-1</sup> ) total/micro-	Pore size distribution(nm) micro-/meso-
Compound I	353.2/57.22	0.357/0.027	1.98/3.56,5.01
Compound II	212.5/0	0.385/0	-/3.68,5.01

Table. S6 Elemental analytical content of CNH.

Compound II	C	N	H
Theoretical	70.7	7.99	7.62
Experimental	74	3.08	5.6

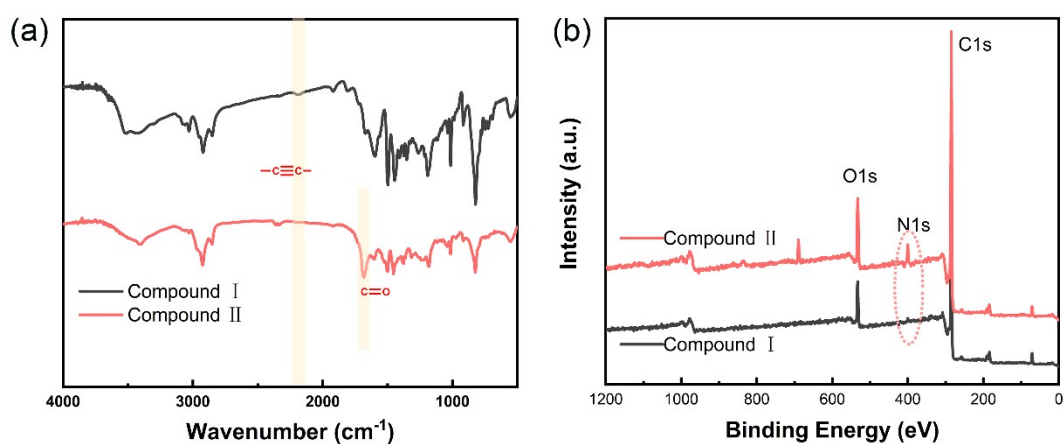


Figure. S15 IR and XPS of Compound I and Compound II.

### 6. Catalysis performance of Compound II

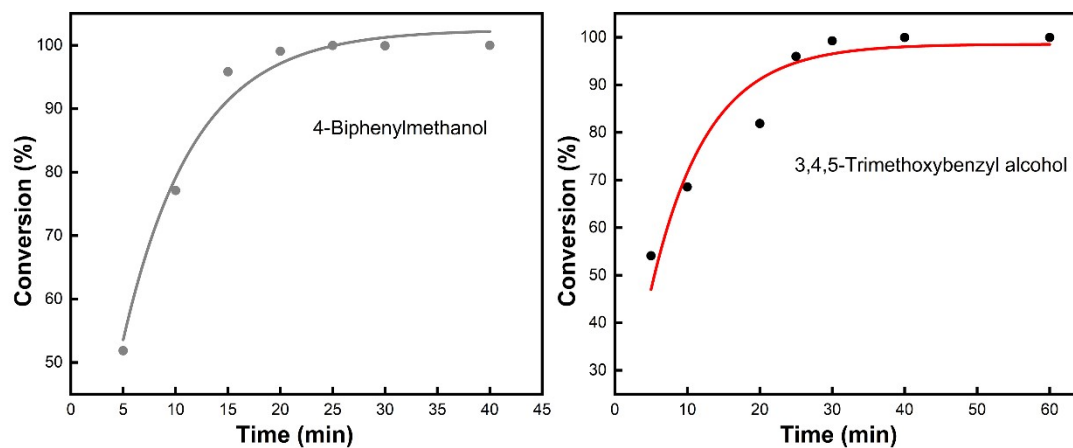
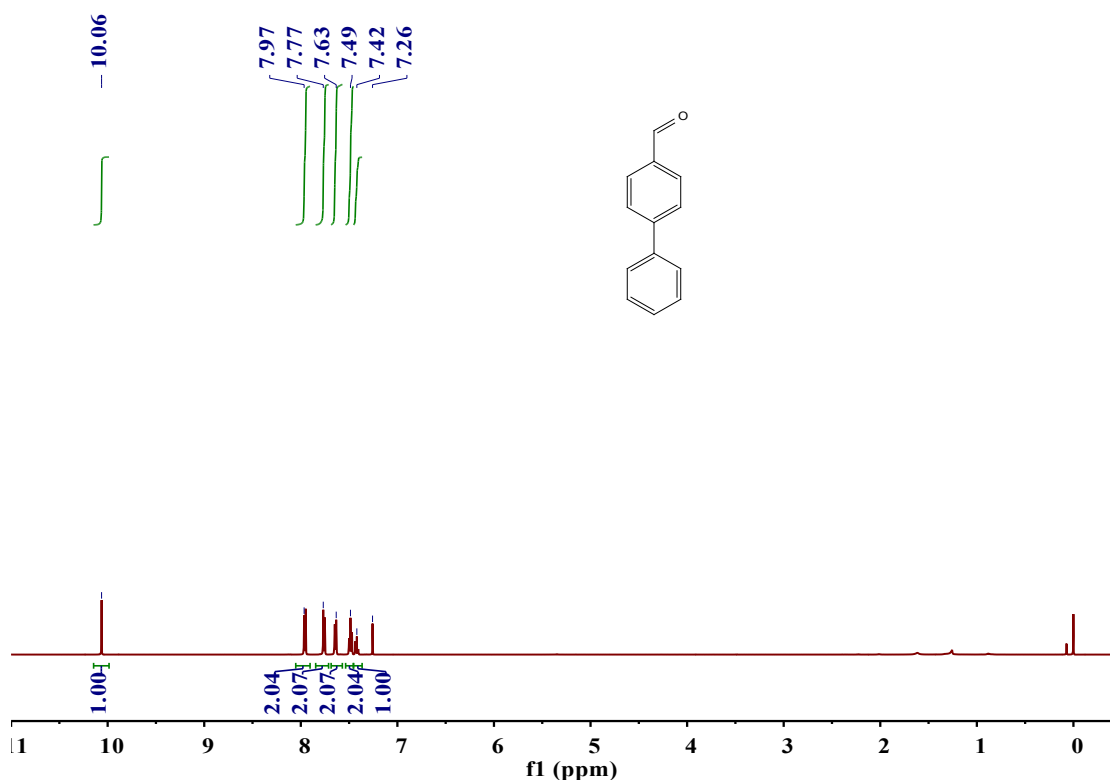


Figure. S16 Conversion curves of Compound II to alcohols.

## 7. $^1\text{H}$ NMR spectra of organic compound



**Figure. S17**  $^1\text{H}$  NMR Spectra for 4-Biphenylcarboxaldehyde (500 MHz,  $\text{CDCl}_3$ ).

The reaction mixture of 5.0 mL of anhydrous acetic acid, 4-biphenylmethanol (223 mg, 1.2 mmol), 1,3-dibromo-5,5-dimethylhydantoin (DBDMH, 25.6 mg),  $\text{NaNO}_2$  (25 mg, 30.0 mol%), and PAF-279 (76 mg), was stirred at 45°C under oxygen atmosphere. The reaction solution is quenched by adding saturated potassium carbonate solution and filtered to remove the solid catalyst. The organic phase was extracted with dichloromethane. After drying on anhydrous sodium sulfate, the crude product was further purified by silica gel column chromatography ( petroleum ether : ethyl acetate = 5 : 1 ).

$$\text{Isolated yield} = \frac{(157.1399 - 156.9324)}{0.22} = 94.3\%$$

## 8. GC spectra and mass spectrometry

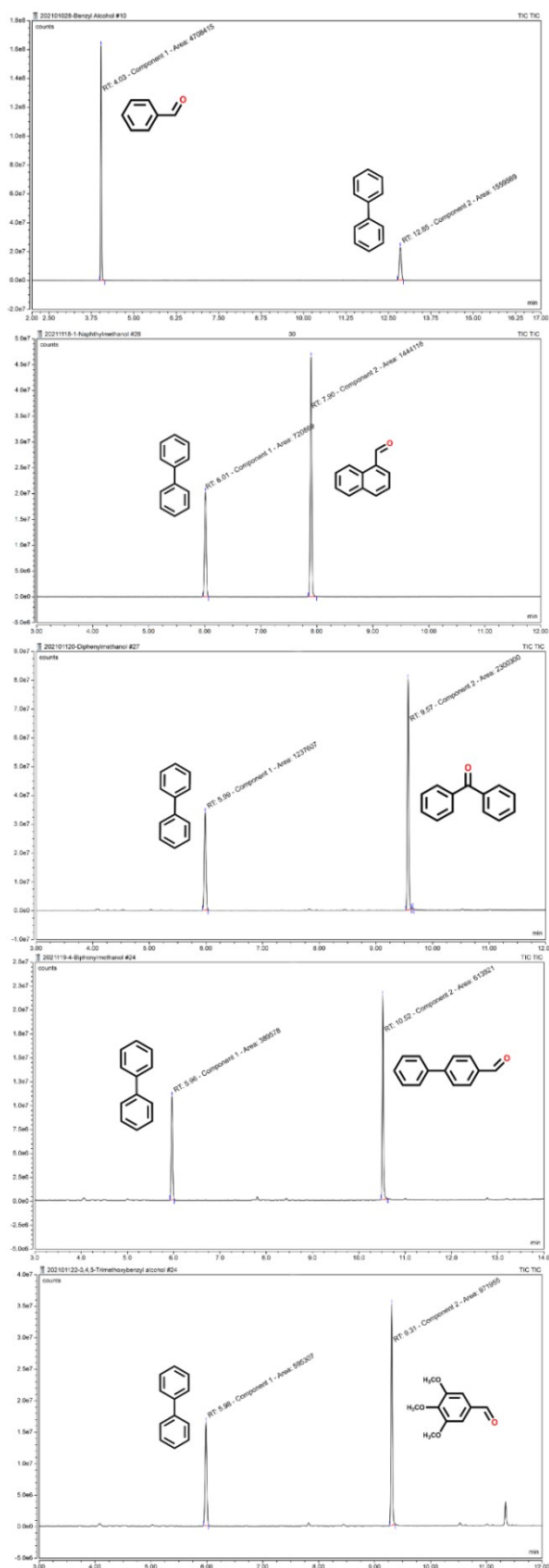


**Figure. S18** Conversion and Selectivity was determined by GC with gas chromatography column.

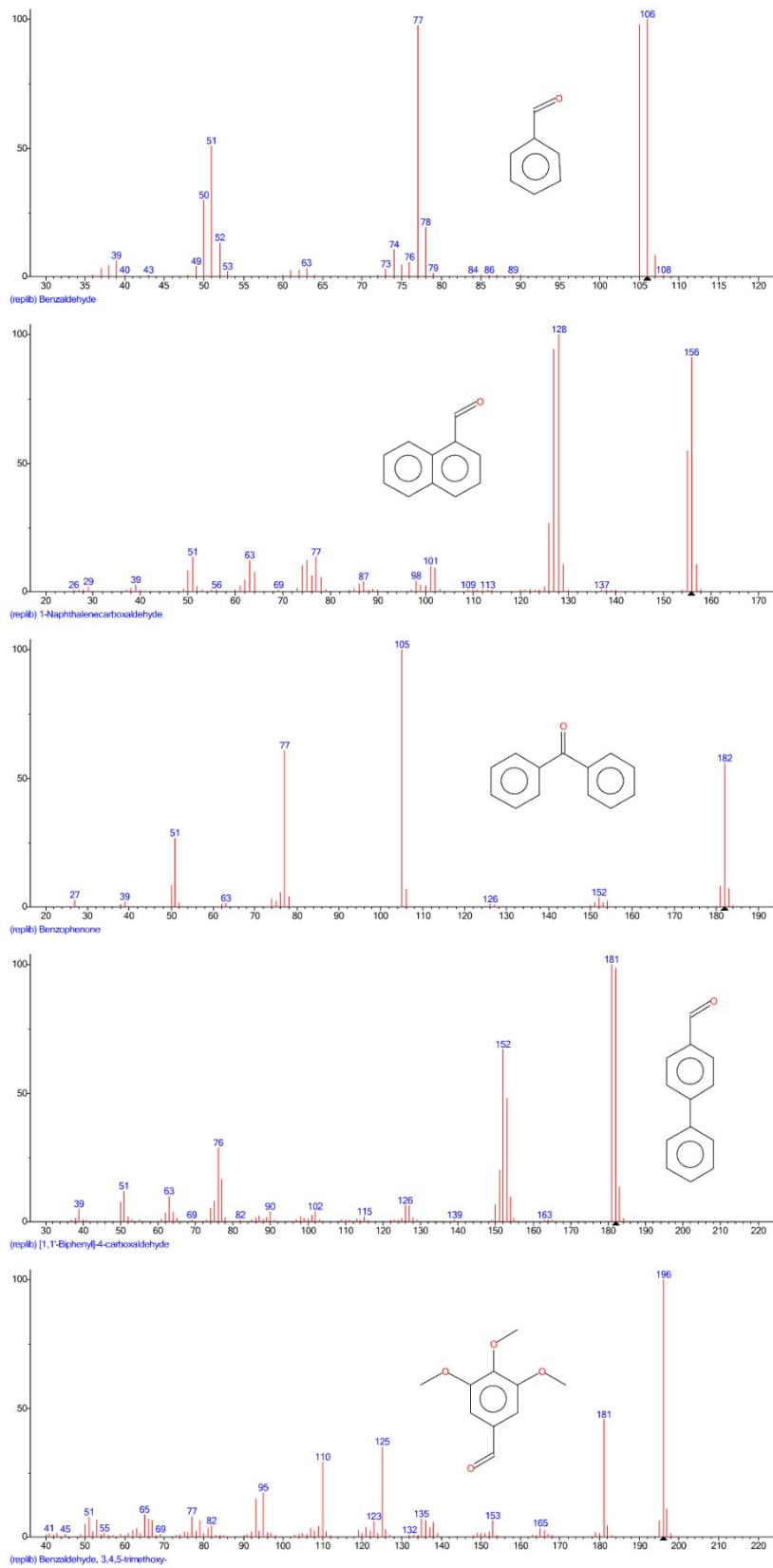


Figure. S19 Mass spectrometry of aldehydes.

1. F. Chen, X. Guan, H. Li, J. Ding, L. Zhu, B. Tang, V. Valtchev, Y. Yan, S. Qiu and Q. Fang, *Angew. Chem. Int. Ed.*, 2021, **60**, 22230-22235.
2. B. Karimi and E. Farhangi, *Chem. Sci.*, 2011, **17**, 6056-6060.
3. B. Karimi, E. Farhangi, H. Vali and S. Vahdati, *ChemSusChem*, 2014, **7**, 2735-2741.
4. R. Liu, X. Liang, C. Dong and X. Hu, *J. Am. Chem. Soc.*, 2004, **126**, 4112-4113.
5. B. Karimi, A. Biglari, J. H. Clark and V. Budarin, *Angew. Chem. Int. Ed.*, 2007, **46**, 7210-7213.
6. M. Liu, B. Zhou, L. Zhou, Z. Xie, S. Li and L. Chen, *J. Mater. Chem. A*, 2018, **6**, 9860-9865.
7. B. Karimi and E. Badreh, *Org. Biomol. Chem*, 2011, **9**, 4194-4198.
8. Y. Shi, Y. Nabae, T. Hayakawa and M.-a. Kakimoto, *RSC Adv.*, 2015, **5**, 1923-1928.
9. A. K. Tucker-Schwartz and R. L. Garrell, *Chem. Eur. J.*, 2010, **16**, 12718-12726.
10. K. M. Zwoliński and M. J. Chmielewski, *ACS Appl. Mater*, 2017, **9**, 33956-33967.
11. A. K. Tucker-Schwartz and R. L. Garrell, *Chem. Eur. J.*, 2010, **16**, 12718-12726.
12. J.-L. Zhuang, X.-Y. Liu, Y. Zhang, C. Wang, H.-L. Mao, J. Guo, X. Du, S.-B. Zhu, B. Ren and A. Terfort, *ACS Appl. Mater*, 2019, **11**, 3034-3043.
13. L. Li, R. Matsuda, I. Tanaka, H. Sato, P. Kanoo, H. J. Jeon, M. L. Foo, A. Wakamiya, Y. Murata and S. Kitagawa, *J. Am. Chem. Soc.*, 2014, **136**, 7543-7546.
14. Y. Guo, W. D. Wang, S. Li, Y. Zhu, X. Wang, X. Liu and Y. Zhang, *Chem Asian J*, 2021, **16**, 3689-3694.
15. H. Ying, Q. Sun, S. Pan, X. Meng and F.-S. Xiao, *ACS Catal.*, 2015, **5**, 1556-1559.
16. Y.-M. Shen, Y. Xue, M. Yan, H.-L. Mao, H. Cheng, Z. Chen, Z.-W. Sui, S.-B. Zhu, X.-J. Yu and J.-L. Zhuang, *Chem. Commun.*, 2021, **57**, 907-910.
17. H. Ma, H. Ren, X. Zou, F. Sun, Z. Yan, K. Cai, D. Wang and G. Zhu, *J. Mater. Chem. A*, 2013, **1**, 752-758.
18. Z. Yan, Y. Yuan, Y. Tian, D. Zhang and G. Zhu, *Angew. Chem. Int. Ed.*, 2015, **54**, 12733-12737.